THE ASTROPHYSICAL JOURNAL, 548:473–481, 2001 February 10

NOTE ON AN EXACT SOLUTION FOR MAGNETOATMOSPHERIC WAVES

P. S. CALLY
Department of Mathematics and Statistics, Monash University, P.O. Box 28M, Victoria, Australia 3800; paul.cally@sci.monash.edu.au
Received 2000 June 13; accepted 2000 September 7

ABSTRACT

Solutions for magnetoatmospheric waves in an isothermal plane stratified atmosphere with uniform vertical magnetic field have long been known in terms of Meijer G-functions. It is pointed out that they may alternatively be expressed using the more familiar hypergeometric ${}_2F_3$ functions, with significant advantages for ease of use and physical interpretation. The nature of these solutions in different regions of the frequency-wavenumber plane is fully discussed, with particular reference to reflection, transmission, and mode conversion. Reflection, transmission, and mode conversion coefficients for slow and fast waves incident from below, including the effects of tunnelling, are calculated exactly. The exact solutions are useful in interpreting observational results and numerical simulations of more complex magnetoatmospheric waves.

Subject headings: MHD — Sun: atmosphere — waves

1. INTRODUCTION

Waves in the solar atmosphere have frequently been modeled, at least in part, as linear magnetohydrodynamic oscillations in a gravitationally plane stratified isothermal atmosphere permeated by a uniform vertical magnetic field (see the review by Thomas 1983). Although not entirely realistic, this model bears sufficient resemblance to certain solar features (e.g., the atmosphere above sunspot umbrae) that it is a useful first step. Indeed, it can be instructive even for more complex magnetic geometries if gravitational stratification is a dominant feature. The model's utility was enhanced by the observation by Zhugzhda & Dzhalilov (1982; see also Zhugzhda 1979) that these oscillations could be fully expressed in terms of Meijer G-functions, specifically G_{24}^{12}. Unfortunately, Meijer functions are at once the most obscure and difficult to use of all the special functions, and furthermore software for evaluating them numerically has only recently become widely available. These facts have limited the extent to which the exact solutions have been used in practice.

However, as was not readily apparent to many, G_{24}^{12} is considerably more elementary than the general Meijer function G_{pq}^{mn} (the nonstandard notation for the G-function adopted by Zhugzhda & Dzhalilov 1982 added to the confusion). In fact, it may always be expressed in terms of the more familiar hypergeometric ${}_2F_3$ functions:

$$G_{2\,4}^{1\,2}\left(x\,\middle|\,\begin{matrix}a_1, & a_2, & \\ b_1, b_2 & b_3, b_4\end{matrix}\right)=\frac{\prod_{j=1}^{2}\Gamma(1-a_j+b_1)}{\prod_{j=2}^{4}\Gamma(1-b_j+b_1)}\,x^{b_1}$$
$$\times\,{}_2F_3(1-a_1+b_1,1-a_2+b_1;1-b_2+b_1,1-b_3+b_1,1-b_4+b_1;-x)\,. \qquad (1)$$

These are easy to work with and easy to evaluate numerically. It is therefore unfortunate that the comparatively elementary nature of the solutions was masked by their formulation in terms of Meijer G-functions.

One purpose of this paper, therefore, is to rework the solutions using hypergeometric functions throughout, with no reference to Meijer functions, so as to make the theory more accessible. We also adopt different notations for the coefficients occurring in the solutions, as these simplify physical interpretation in terms of well-understood acoustic-gravity waves in the two asymptotic regimes[1] $\beta\to 0$ and $\beta\to\infty$. We must emphasize though that our solutions are not any more complete or correct than the Meijer G solutions. There is nothing in this paper that could not be derived in principle using those functions. Indeed, many of the results presented here are also to be found in Zhugzhda & Dzhalilov (1982).

Finally, as well as pointing out the more elementary form of the solutions, we also take the opportunity to complete the discussion of reflection and transmission coefficients in Zhugzhda & Dzhalilov by including the effect of fast mode tunnelling in the lower atmosphere, which allows evanescent waves to carry energy upward.

2. EQUATIONS AND SOLUTIONS

Without loss of generality, we consider waves propagating in the x-z plane, with a time and horizontal dependence of the form $\exp[i(kx-\omega t)]$ assumed. The governing linearized adiabatic ideal MHD oscillation equations are then of sixth order. However, the magnetoacoustic-gravity waves (fourth order, with fluid velocity $u\boldsymbol{i}+w\boldsymbol{k}$ purely in the x-z plane) and the transverse Alfvén waves (second order, velocity $v\boldsymbol{j}$) decouple. The magnetoacoustic-gravity wave equation was given by Zhugzhda & Dzhalilov (1982) as a single fourth order ordinary differential equation for u. Adopting different notations, this may be written as

$$\zeta^4u^{(4)}+4\zeta^3u'''+\zeta^2(2-4\kappa^2+4\kappa_0^2+4\zeta^2)u''+4\zeta(\kappa^2+\kappa_0^2+3\zeta^2)u'+4[(4\kappa_z^2+1)\zeta^2-4\kappa_0^2\kappa^2-\kappa^2]u=0\,. \qquad (2)$$

[1] The plasma β is defined as the ratio of the gas and the magnetic pressure. In terms of the sound and Alfvén speeds c and a, respectively, $\beta=2c^2/(\gamma a^2)$, where γ is the adiabatic index.

Here $\nu = \omega H/c$ is a dimensionless frequency and $\kappa = kH$ a dimensionless wavenumber, where H is the (constant) density scale height and c is the adiabatic sound speed (*not* the isothermal sound speed, as is the notation in Zhugzhda & Dzhalilov 1982). Vertical position is represented by $\zeta = \omega H/a$, where a is the Alfvén speed. Note that $a \propto e^{z/2H}$ (where z is the height), so that ζ *decreases* with increasing z such that the limit $z \to \infty$ corresponds to $\zeta \to 0^+$. The primes on u represent derivatives with respect to ζ. Setting $n = NH/c$, where $N = (\gamma - 1)^{1/2}c/\gamma H$ is the Brunt-Väisälä frequency, we have defined

$$\kappa_z = \sqrt{\nu^2 + (n^2 - \nu^2)\kappa^2/\nu^2 - \tfrac{1}{4}} \tag{3a}$$

and

$$\kappa_0 = \sqrt{\nu^2 - \tfrac{1}{4}}\ . \tag{3b}$$

In a uniform magnetofluid, the magnetoacoustic oscillations may be classed as either "fast" or "slow" (Ferraro & Plumpton 1966), depending on their phase speed. This classification is at best useful only locally in a stratified fluid. An exact normal mode of this system may be fast in some regions and slow in others, or, as we shall see, may contain a mixture of both fast and slow. However, in practice, it is often important to keep track of how the fast and slow waves reflect or couple as they propagate through the inhomogeneous region. The exact solutions we present here provide useful insights into these processes since their asymptotic behaviors in the regions $a \gg c$ and $a \ll c$ are easily identified with the classical fast and slow waves.

The significance of κ_z as defined by equation (3a) is that it is the vertical dimensionless wavenumber in an isothermal atmosphere *without* magnetic field. In that case, the acoustic-gravity wave dispersion relation is (Lamb 1945)

$$\nu^4 - \nu^2(\kappa^2 + \kappa_z^2 + \tfrac{1}{4}) + \kappa^2 n^2 = 0\ . \tag{4}$$

The known acoustic-gravity solutions are then

$$u_{ag} = \exp(z/2H)\exp(\pm i k_z z) \propto \zeta^{-1 \mp 2i\kappa_z}\ , \tag{5}$$

which therefore is the expected fast mode velocity where $a \ll c$. The propagation diagram, Figure 1, shows where in the κ-ν plane these waves are vertically propagating ($\kappa_z^2 > 0$: Regions I and II) and where they are evanescent ($\kappa_z^2 < 0$: Regions III and IV). κ_0 is then the value of κ_z if the wave is purely vertical, i.e., $\kappa = 0$. The parameters κ_z and κ_0 take important roles in the exact solution for *magneto*-acoustic-gravity waves.

Equation (2) describes the magnetoatmospheric waves only. The (entirely transverse) Alfvén modes decouple and admit the solution for the y-component of velocity v in terms of Bessel functions (Ferraro & Plumpton 1958)

$$v_A = \mathscr{A} J_0(2\zeta) + \mathscr{B} Y_0(2\zeta)\ .$$

If ζ extends to 0, then clearly $\mathscr{B} = 0$ must be selected. We shall not be directly concerned with Alfvén waves, but note the following for future reference.

1. For $a \ll c$ in an unstratified medium, the slow wave dispersion relation reduces to that for Alfvén waves, $\omega = ak_z$, where k_z is the wavenumber in the direction of the field lines. In this limit, the group velocity has collapsed to be purely vertical, just

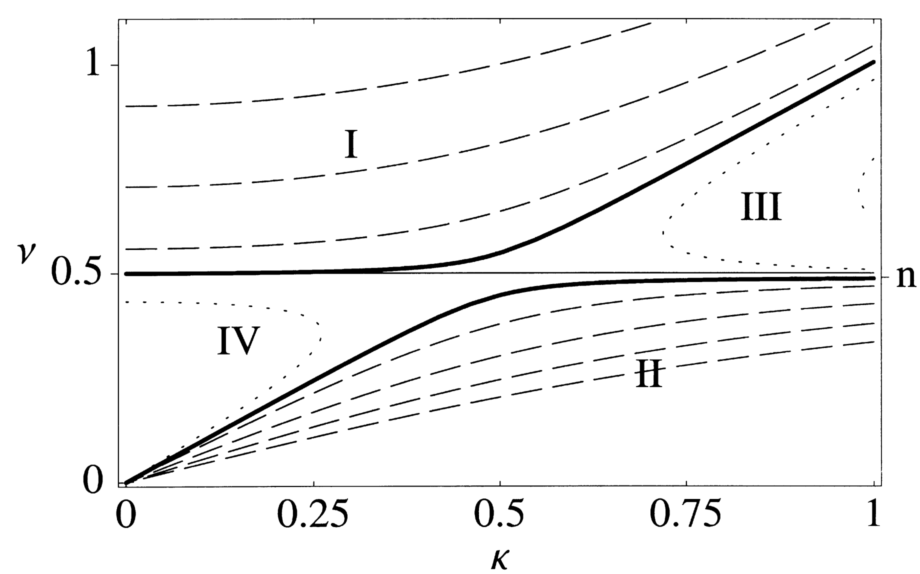

FIG. 1.—Propagation diagram for acoustic-gravity waves with $\gamma = 5/3$ ($n = 0.4899$). In regions I (acoustic) and II (gravity) the waves are vertically propagating ($\kappa_z^2 > 0$), whereas they are evanescent in Regions III and IV ($\kappa_z^2 < 0$). $\kappa_z = 0$ on the heavy curves, $\kappa_z = 0.25$, 0.5, 0.75, and 1 on the dashed curves (increasing away from the heavy lines), and $\kappa_z = 0.25i$ and $0.5i$ on the dotted curves. The acoustic cutoff $\nu = \frac{1}{2}$ is shown as a thin full line. The distinction between III and IV is that a purely vertical mode ($\kappa = 0$) is vertically propagating in the former but evanescent in the latter.

as for the Alfvén wave. Furthermore, in the stratified medium, the vertical wavelength is much less that the scale height, $2\pi\omega/a \ll H$, and so the unstratified results apply there in the WKB sense. We therefore conclude that the slow and Alfvén solutions are essentially identical in this limit (the polarization is irrelevant because propagation is purely vertical).

2. The large ζ asymptotic formula is (with $\mathscr{A}^2 + \mathscr{B}^2 = 1$)

$$v_{\rm A} = \frac{1}{\sqrt{\pi\zeta}}\,[\cos(2\zeta - \phi) + O(\zeta^{-1})]\;, \tag{6}$$

where ϕ is a phase constant.

The slow mode in the high β region should therefore have this asymptotic behavior for u.

The general solution of equation (2) may be written in terms of the hypergeometric ${}_2F_3$ function (Luke 1975), defined for all complex x by the rapidly convergent series

$${}_2F_3(a_1, a_2; b_1, b_2, b_3; x) = \sum_{n=0}^{\infty} \frac{(a_1)_n (a_2)_n}{(b_1)_n (b_2)_n (b_3)_n} \frac{x^n}{n!}\;, \tag{7}$$

where $(a)_0 = 1$, $(a)_n = a(a+1)\ldots(a+n-1)$ is the Pochhammer symbol. We find

$$\begin{aligned} u = {} & C_1 \zeta^{-2\kappa} {}_2F_3(\tfrac{1}{2} - \kappa - i\kappa_z, \tfrac{1}{2} - \kappa + i\kappa_z; 1 - 2\kappa, \tfrac{1}{2} - \kappa - i\kappa_0, \tfrac{1}{2} - \kappa + i\kappa_0; -\zeta^2) \\ & + C_2 \zeta^{2\kappa} {}_2F_3(\tfrac{1}{2} + \kappa - i\kappa_z, \tfrac{1}{2} + \kappa + i\kappa_z; 1 + 2\kappa, \tfrac{1}{2} + \kappa - i\kappa_0, \tfrac{1}{2} + \kappa + i\kappa_0; -\zeta^2) \\ & + C_3 \zeta^{1-2i\kappa_0} {}_2F_3(1 - i\kappa_0 - i\kappa_z, 1 - i\kappa_0 + i\kappa_z; 1 - 2i\kappa_0, \tfrac{3}{2} - i\kappa_0 - \kappa, \tfrac{3}{2} - i\kappa_0 + \kappa; -\zeta^2) \\ & + C_4 \zeta^{1+2i\kappa_0} {}_2F_3(1 + i\kappa_0 - i\kappa_z, 1 + i\kappa_0 + i\kappa_z; 1 + 2i\kappa_0, \tfrac{3}{2} + i\kappa_0 - \kappa, \tfrac{3}{2} + i\kappa_0 + \kappa; -\zeta^2)\;, \end{aligned} \tag{8}$$

where the C_i are arbitrary constants with the dimensions of velocity. (The ${}_2F_3$ solutions were noted by Zhugzhda & Dzhalilov 1982, eq. [4], as asymptotic representations of the Meijer functions in the $\zeta \ll 1$ limit, but they did not recognize that they are valid for all ζ.) These solutions have been verified using the computer algebra package "Mathematica" (Wolfram 1999). The vertical velocity w subsequently follows from

$$w = \frac{i\nu^2}{8\gamma\zeta^2\kappa(\nu^2 - n^2)}\left[\gamma\zeta^3 u''' + (3\gamma - 2)\zeta^2 u'' + (4\gamma\zeta^2 - 4\gamma\kappa^2 + \gamma - 2)\zeta u' + 8((\gamma - 1)\zeta^2 + \kappa^2)u\right]. \tag{9}$$

We denote the four solutions (without the C coefficients) by u_1, u_2, u_3, and u_4, respectively, and similarly for w, and refer to them as type 1, type 2, type 3, and type 4 solutions.

The general solution (eq. [8]) is surprisingly concise and suggestive, given the complexity of the differential equation (2). In particular, its constituent parameters κ_z and κ_0 clearly refer to the acoustic-gravity solution in the high β region and the vertically propagating sound wave in the low β regime, respectively. In the next section, we show that these waves appear naturally and easily in these asymptotic limits, as do the magnetic solutions.

3. ASYMPTOTIC BEHAVIORS

3.1. *Low β Regime*

The ${}_2F_3$ function as defined by equation (7) is almost elementary. In particular, for an unbounded atmosphere, where $\zeta \to 0$ as $z \to \infty$, the low β asymptotic behavior follows directly from equation (7):

$${}_2F_3(a_1, a_2; b_1, b_2, b_3; -\zeta^2) = 1 + O(\zeta^2)\;.$$

The four leading asymptotic behaviors are then simply $\zeta^{-2\kappa}$, $\zeta^{2\kappa}$, $\zeta^{1-2i\kappa_0}$, and $\zeta^{1+2i\kappa_0}$, or, in terms of z,

$$\zeta_0^{\mp 2\kappa} e^{\pm kz} \text{ and } \zeta_0^{1\mp 2i\kappa_0} \exp\left\{-(z/2H)[1 \mp \sqrt{1 - (\omega^2/\omega_c^2)}]\right\}\;, \tag{10}$$

respectively. Here $\omega_c = c/2H$ is the acoustic cutoff frequency ($\nu = \frac{1}{2}$ in our dimensionless units), and ζ_0 is the value of ζ at $z = 0$. These clearly indicate the physical natures of the four solutions at large z, and make application of natural boundary conditions there very straightforward. Assuming $\kappa > 0$, we must set $C_1 = 0$ to dispense with the exponentially growing solution. The remaining C_2 solution is evanescent. Thus, the type 1 and type 2 solutions represent the fast mode at large z, where it is essentially magnetic since $a \gg c$. In that limit, the fast wave dispersion relation is $k^2 + k_z^2 = \omega^2/a^2 \to 0$, where k_z is the vertical wavenumber, i.e., $k_z = \pm ik$. Hence, the $\zeta^{\mp 2\kappa}$ (i.e., $e^{\pm kz}$) behaviors.

The type 3 and type 4 solutions, however, are predominantly acoustic at large height, and strongly channeled in the vertical direction by the magnetic field of the low β plasma (it is easily verified that $u/w = O(\zeta^2)$ in this limit). In Regions I and III, where κ_0 is real (and by assumption positive), the type 3 solution represents and outgoing wave, and the type 4 an incoming wave. On the other hand, in Regions II and IV (arg $\kappa_0 = \pi/2$), the kinetic energy density of the type 3 solution decays exponentially with increasing height, whereas for type 4 it grows exponentially. In either case, the physical solution is type 3, i.e., we must set $C_4 = 0$.

3.2. *High β Regime*

Asymptotic expansions of the ${}_2F_3$ functions are also available for large ζ, i.e., $a \ll c$, (Luke 1975, § 5.9.3). The appropriate relation for our purposes is

$$
\begin{aligned}
{}_2F_3(a_1, a_2; b_1, b_2, b_3; -\zeta^2) = \frac{\Gamma(b_1)\Gamma(b_2)\Gamma(b_3)}{\Gamma(a_1)\Gamma(a_2)} \Bigg\{ & \frac{\zeta^\lambda}{\sqrt{\pi}} \left[\cos\left(2\zeta + \frac{1}{2}\lambda\pi\right) + O(\zeta^{-1}) \right] \\
& + \frac{\Gamma(a_1)\Gamma(a_2 - a_1)}{\Gamma(b_1 - a_1)\Gamma(b_2 - a_1)\Gamma(b_3 - a_1)} \zeta^{-2a_1}[1 + O(\zeta^{-2})] \\
& + \frac{\Gamma(a_2)\Gamma(a_1 - a_2)}{\Gamma(b_1 - a_2)\Gamma(b_2 - a_2)\Gamma(b_3 - a_2)} \zeta^{-2a_2}[1 + O(\zeta^{-2})] \Bigg\}
\end{aligned}
\tag{11}
$$

as $\zeta \to \infty$, where $\lambda = \frac{1}{2} + \sum_{i=1}^{2} a_i - \sum_{i=1}^{3} b_i$.

Equation (11) may be used to determine the asymptotic natures of the four solutions at high β. To leading order,

$$
u_j \sim a_{1\,j}\zeta^{-1/2}e^{2i\zeta} + a_{2\,j}\zeta^{-1/2}e^{-2i\zeta} + a_{3j}\zeta^{-1+2i\kappa_z} + a_{4\,j}\zeta^{-1-2i\kappa_z} , \tag{12}
$$

$(j = 1, \ldots, 4)$, as $\zeta \to \infty$. Applying this to the u_2 solution, for which $\lambda = -\frac{1}{2} - 2\kappa$, we find

$$
a_{1\,2}, a_{2\,2} = \frac{\Gamma(1 + 2\kappa)\Gamma(1/2 + \kappa + i\kappa_0)\Gamma(1/2 + \kappa - i\kappa_0)}{2\sqrt{\pi}\Gamma(1/2 + \kappa + i\kappa_z)\Gamma(1/2 + \kappa - i\kappa_z)} e^{\mp i\pi(\kappa + 1/4)}
$$

and

$$
a_{3\,2}, a_{4\,2} = \frac{\Gamma(1 + 2\kappa)\Gamma(1/2 + \kappa + i\kappa_0)\Gamma(1/2 + \kappa - i\kappa_0)\Gamma(\pm 2i\kappa_z)}{\Gamma(1/2 + \kappa \pm i\kappa_z)^2\Gamma(\pm i\kappa_z - i\kappa_0)\Gamma(\pm i\kappa_z + i\kappa_0)} .
$$

In each case, the first-named a coefficient on the left-hand side corresponds to the upper sign on the right-hand side. On the other hand, for the type 3 solution (where $\lambda = -\frac{3}{2} + 2i\kappa_0$)

$$
a_{1\,3}, a_{2\,3} = \frac{\Gamma(1 - 2i\kappa_0)\Gamma(3/2 - \kappa - i\kappa_0)\Gamma(3/2 + \kappa - i\kappa_0)}{2\sqrt{\pi}\Gamma(1 - i\kappa_0 - i\kappa_z)\Gamma(1 - i\kappa_0 + i\kappa_z)} e^{\mp \pi(\kappa_0 + 3i/4)}
$$

and

$$
a_{3\,3}, a_{4\,3} = \frac{\Gamma(1 - 2i\kappa_0)\Gamma(3/2 - \kappa - i\kappa_0)\Gamma(3/2 + \kappa - i\kappa_0)\Gamma(\pm 2i\kappa_z)}{\Gamma(\pm i\kappa_z - i\kappa_0)\Gamma(1/2 - \kappa \pm i\kappa_z)\Gamma(1/2 + \kappa \pm i\kappa_z)\Gamma(1 - i\kappa_0 \pm i\kappa_z)} .
$$

The a_{k1} coefficients are the same as the a_{k2}, but with the sign of κ reversed. The a_{k4} are as for a_{k3}, but with κ_0 reversed. Reference to equations (6) and (5) indicate that the first two terms on the right-hand side of equation (12) represent the slow modes locally and the last two terms are the fast modes.

We now consider each of the four regions of the propagation diagram in turn.

I. Here $\kappa_z > 0$ and $\kappa_0 > 0$. Both slow and fast waves are propagating. In the type 2 mode, since the upward and downward amplitudes for each are equal, they are both standing waves. This is consistent with type 2 being evanescent at large z. On the other hand, the amplitudes of the upward propagating fast and slow waves at low z exceed those of the downward propagating modes, i.e., the waves are only partly reflected.

II. Here $\kappa_z > 0$ and κ_0 is imaginary ($\mathrm{Im}\kappa_0 > 0$). Both fast and slow waves are standing for each of type 2 and type 3 solutions.

III. Here κ_z is imaginary ($\mathrm{Im}\kappa_z > 0$) and $\kappa_0 > 0$. The fast wave is evanescent. For type 2, the slow wave is standing. It is partially reflected in the type 3 solution.

IV. Here both κ_z and κ_0 are imaginary ($\mathrm{Im}\kappa_0 > 0$, $\mathrm{Im}\kappa_z > 0$). The fast wave is evanescent and the slow wave standing for each of type 2 and type 3 solutions.

4. ENERGY TRANSPORT AND MODE CONVERSION

The time-averaged wave-energy flux is made up of acoustic and magnetic components (Bray & Loughhead 1974, p. 252),

$$
\boldsymbol{F} = \frac{1}{2}\,\mathrm{Re}\left\{ p_1\bar{\boldsymbol{v}} - \frac{1}{\mu}(\bar{\boldsymbol{v}} \times \boldsymbol{B}_0) \times \boldsymbol{B}_1 \right\} ,
$$

where $\boldsymbol{v} = (u, 0, w)$ is the vector velocity, p_1 the Eulerian pressure perturbation, $\boldsymbol{B}_0$ the background uniform magnetic field, $\boldsymbol{B}_1$ the perturbation to the field, and μ the magnetic permeability. In terms of our dimensionless variables, the vertical component is

$$
F_z = \frac{p_{\mathrm{mag}}}{c}\,\mathrm{Re}\left\{ i\zeta^2\nu^{-3}\left(\gamma^{-1}w - i\kappa u + \frac{1}{2}\zeta w'\right)\bar{w} + i\,\frac{1}{2}\,\nu^{-1}\zeta u'\bar{u} \right\} , \tag{13}
$$

where p_{mag} is the magnetic pressure. We shall neglect the factor p_{mag}/c from now on. It may be confirmed that equation (13) yields a flux independent of ζ for each of the four normal modes. Indeed, $F_z = 0$ for type 1 and type 2, $F_z = \phi\mathscr{U}(\kappa_0^2)$ for type 3, where $\mathscr{U}$ is the unit step function and

$$\phi = \frac{\kappa_0 \nu[(\kappa^2 + \nu^2)^2 - \kappa^2]}{\kappa^2(\nu^2 - n^2)} , \tag{14}$$

and $F_z = -\phi\mathscr{U}(\kappa_0^2)$ for the type 4 solution. These are consistent with the pure asymptotic behaviors at low β. However, there are also cross-terms of the types 1 and 2 solutions, resulting from $u_1' \bar{u}_2$ and $u_2' \bar{u}_1$ in equation (13). The respective contributions to the flux are $-i\nu\kappa$ and $i\nu\kappa$. Of course these are of no concern if the isothermal atmosphere extends indefinitely upward, since then the u_1 solution must be dropped. However, it will be present in a finite layer such as the chromosphere, and even if $\zeta \ll 1$ there and u_1 and u_2 take the asymptotic forms set out in equation (10), energy is carried upward by them in combination. This is the effect of tunnelling. Similarly, there are cross-terms of the type 3 and 4 solutions: $\phi\mathscr{U}(-\kappa_0^2)$ results from the $w_3' \bar{w}_4$ term, and $-\phi\mathscr{U}(-\kappa_0^2)$ from the one involving $w_4' \bar{w}_3$. Note that ϕ is pure imaginary where $\kappa_0^2 < 0$. These are the only cross-terms. Representing the flux associated with solution u by $\mathscr{F}[u]$, these results may be represented as a Hermitian form:

$$F_z = \mathscr{F}[C_1 u_1 + C_2 u_2 + C_3 u_3 + C_4 u_4] = C^H \Phi C ,$$

where $C = (C_1, C_2, C_3, C_4)^T$, the superscript H indicates the Hermitian transpose, and

$$\Phi = \begin{bmatrix} 0 & i\kappa\nu^{-1} & 0 & 0 \\ -i\kappa\nu^{-1} & 0 & 0 & 0 \\ 0 & 0 & \phi\mathscr{U}(\kappa_0^2) & -\phi\mathscr{U}(-\kappa_0^2) \\ 0 & 0 & \phi\mathscr{U}(-\kappa_0^2) & -\phi\mathscr{U}(\kappa_0^2) \end{bmatrix} . \tag{15}$$

We may of course employ any linearly independent combination of the u_i as a solution basis. One obvious choice is the set with asymptotic behaviors $u \sim \zeta^{-1/2} e^{\mp 2i\zeta}$ and $u \sim \zeta^{-1 \mp 2i\kappa_z}$ as $\zeta \to \infty$ (cf. eq. [12]). If

$$u \sim c_1 \zeta^{-1/2} e^{2i\zeta} + c_2 \zeta^{-1/2} e^{-2i\zeta} + c_3 \zeta^{-1+2i\kappa_z} + c_4 \zeta^{-1-2i\kappa_z} \tag{16}$$

in that limit, then the C and the c coefficients are related by $c = AC$, where $c = (c_1, c_2, c_3, c_4)^T$ and A is the 4×4 matrix (a_{jk}). An alternate equation for the vertical flux is therefore

$$F_z = c^H \Psi c , \tag{17}$$

where $\Psi = A^{-H} \Phi A^{-1}$ is given concisely by

$$\Psi = \begin{bmatrix} -\nu^{-1} & & 0 & 0 \\ 0 & \nu^{-1} & 0 & 0 \\ 0 & 0 & -f\mathscr{U}(\kappa_z^2) & f\mathscr{U}(-\kappa_z^2) \\ 0 & 0 & -f\mathscr{U}(-\kappa_z^2) & f\mathscr{U}(\kappa_z^2) \end{bmatrix} , \tag{18}$$

where

$$f = \frac{\nu\kappa_z}{\kappa^2(\nu^2 - n^2)} .$$

The term ν^{-1} represents the vertical flux carried by the pure slow mode in the limit $\zeta \to 0$. On the other hand, f is the fast mode flux in this limit. Note that $f > 0$ in Region I, $f < 0$ in Region II, $\arg f = \pi/2$ in Region III, and $\arg f = -\pi/2$ in Region IV. That f is negative in Region II is due to the well-known feature of gravity waves that the vertical components of phase and group velocity have opposite signs. In Regions III and IV the fast mode is evanescent at high β, but energy may nonetheless be carried by tunnelling if $c_3 \bar{c}_4$ has a nonzero imaginary part.

4.1. *Reflection, Transmission, and Conversion Coefficients*

In their classic paper, Zhugzhda & Dzhalilov (1982) presented a near-complete survey of reflection and transmission coefficients in the four regions of the propagation diagram. Only the effect of fast mode tunnelling in Regions III and IV was left out. We correct that omission here and take the opportunity to set out the complete picture.

4.1.1. *Incident Slow Mode*

With the asymptotic expressions (eq. [16]) in mind, a physical solution which has only a slow wave incident from high β is

$$u_s = a_{43} u_2 - a_{42} u_3 , \tag{19a}$$

in Regions I, III, and IV, or

$$u_s = a_{33} u_2 - a_{32} u_3 , \tag{19b}$$

in Region II. In Regions III and IV, where the fast wave is evanescent, it is appropriate to retain only the fast mode solution which decreases *downward*, i.e., which is a surface wave on the $\beta \approx 1$ layer, excited by the upgoing slow wave. This is why equation (19a) is selected there. In general, the slow wave will be partially transmitted into the overlying low β region (where it will always take the form of a slow wave, since the fast mode there is evanescent), partially reflected as a downgoing slow wave, and partially converted into a downgoing fast wave. Table 1 lists incident, reflected, and converted energy fluxes. In Region III, where $f = i|f|$ and the fast mode terms in Ψ are off-diagonal, the total flux as given by equation (18) is $-|c_1|^2 \nu^{-1} + |c_2|^2 \nu^{-1} - \frac{1}{2}|c_3 - ic_4|^2 |f| + \frac{1}{2}|c_3 + ic_4|^2 |f|$. These terms are therefore identified as the downward and

TABLE 1

INCIDENT, REFLECTED, AND CONVERTED ENERGY FLUXES FOR SLOW AND FAST MODES INCIDENT FROM BELOW

		SLOW			FAST		
REGION	f	F_{inc}	F_{ref}	F_{conv}	F_{inc}	F_{ref}	F_{conv}
I........	>0	$\lvert c_2\rvert^2/\nu$	$\lvert c_1\rvert^2/\nu$	$\lvert c_3\rvert^2 f$	$\lvert c_4\rvert^2 f$	$\lvert c_3\rvert^2 f$	$\lvert c_1\rvert^2/\nu$
II.......	<0	$\lvert c_2\rvert^2/\nu$	$\lvert c_1\rvert^2/\nu$	$\lvert c_4\rvert^2\lvert f\rvert$	$\lvert c_3\rvert^2\lvert f\rvert$	$\lvert c_4\rvert^2\lvert f\rvert$	$\lvert c_1\rvert^2/\nu$
III......	$i\lvert f\rvert$	$\lvert c_2\rvert^2/\nu$	$\lvert c_1\rvert^2/\nu$	0	$\frac{1}{2}\lvert c_3+ic_4\rvert^2\lvert f\rvert$	$\frac{1}{2}\lvert c_3-ic_4\rvert^2\lvert f\rvert$	$\lvert c_1\rvert^2/\nu$
IV......	$-i\lvert f\rvert$	$\lvert c_2\rvert^2/\nu$	$\lvert c_1\rvert^2/\nu$	0	$\frac{1}{2}\lvert c_3-ic_4\rvert^2\lvert f\rvert$	$\frac{1}{2}\lvert c_3+ic_4\rvert^2\lvert f\rvert$	$\lvert c_1\rvert^2/\nu$

TABLE 2

REFLECTION, TRANSMISSION, AND CONVERSION COEFFICIENTS FOR A SLOW MODE INCIDENT FROM BELOW

Region	$\mathscr{R}$	$\mathscr{T}$	$\mathscr{C}$
I........	$e^{-4\pi(\kappa_0-\kappa_z)}$	$\dfrac{2\sinh 2\pi\kappa_0 \sinh \pi(\kappa_0-\kappa_z)}{\sinh \pi(\kappa_0+\kappa_z)}\,e^{-2\pi(\kappa_0-\kappa_z)}$	$\dfrac{2\sinh 2\pi\kappa_z \sinh \pi(\kappa_0-\kappa_z)}{\sinh \pi(\kappa_0+\kappa_z)}\,e^{-2\pi(\kappa_0-\kappa_z)}$
II.......	$e^{-4\pi\kappa_z}$	0	$1-e^{-4\pi\kappa_z}$
III......	$e^{-4\pi\kappa_0}$	$1-e^{-4\pi\kappa_0}$	0
IV......	1	0	0

upward slow mode fluxes, and the downward and upward fast mode fluxes, respectively. Since $f = -i\lvert f\rvert$ in Region IV, the identification of the downward and upward fast mode fluxes is reversed there.

The total transmitted flux is the incident flux minus the reflected and converted fluxes,

$$F_{\text{trans}} = F_{\text{inc}} - F_{\text{ref}} - F_{\text{conv}} \, .$$

The reflection, transmission, and conversion coefficients are then defined by

$$\{\mathscr{R}, \mathscr{T}, \mathscr{C}\} = \frac{\{F_{\text{ref}}, F_{\text{trans}}, F_{\text{conv}}\}}{F_{\text{inc}}} \, , \tag{20}$$

where an ordered list notation has been used. Expressions for $\mathscr{T}$, $\mathscr{R}$, and $\mathscr{C}$ may be reduced to simple forms using various gamma function identities and are set out in Table 2 (all in agreement with the results given by Zhugzhda & Dzhalilov 1982). They are also plotted in Figure 2 as a function of κ for various frequencies ν. Above the acoustic cutoff frequency, we see that $\mathscr{T}$ increases monotonically from 0 toward 1 as κ increases from 0, whereas $\mathscr{R}$ decreases from 1 toward 0 over the same range. A non-negligible slow-to-fast mode conversion occurs at intermediate wavenumbers in Region I. In Region III, where of course $\mathscr{C} = 0$ since the fast mode is evanescent, transmission is close to total. Below the cutoff frequency though, $\mathscr{T} = 0$ identically since all available modes in the overlying low β plasma are evanescent. Effectively, slow-slow reflection is total ($\mathscr{R} = 1$) in Region IV, while slow-fast conversion has taken over in Region II.

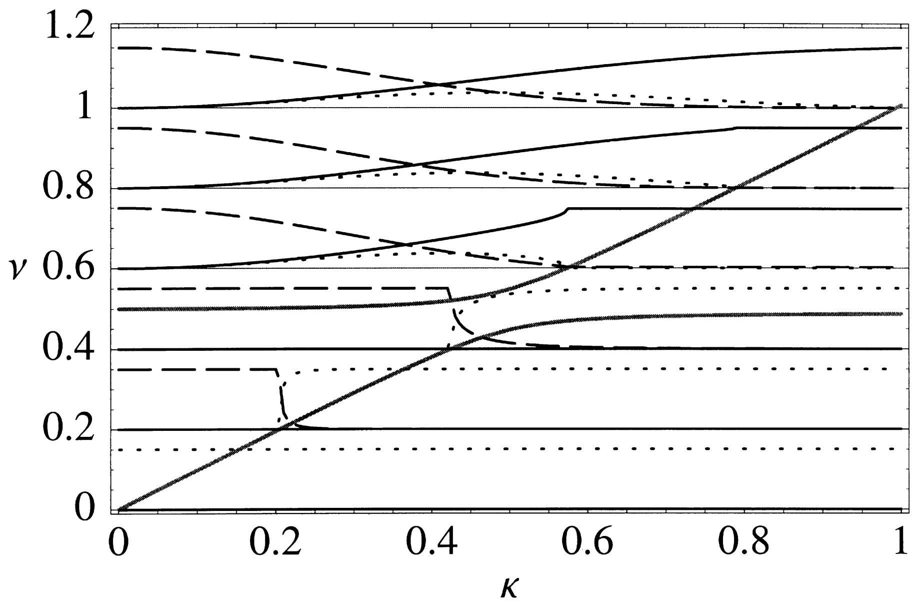

FIG. 2.—The transmission (*solid curves*), reflection (*dashed curves*), and conversion (*dotted curves*) coefficients $\mathscr{T}$, $\mathscr{R}$, and $\mathscr{C}$ for a pure slow mode incident from $z \to -\infty$, as a function of position in the propagation diagram (cf. Fig. 1). The baseline of each graph is placed at its fixed frequency $\nu = 0$, 0.2, 0.4, 0.6, 0.8, and 1.0, and wavenumber κ is varied continuously. The adiabatic index $\gamma = 5/3$.

TABLE 3

Reflection, Transmission, and Conversion Coefficients for a Fast Mode Incident from below

Region	$\mathscr{R}$	$\mathscr{T}$	$\mathscr{C}$
I………	$\dfrac{\sinh^2 \pi(\kappa_0 - \kappa_z)}{\sinh^2 \pi(\kappa_0 + \kappa_z)} e^{4\pi\kappa_z}$	$\left[1 - \dfrac{\sinh^2 \pi(\kappa_0 - \kappa_z)}{\sinh^2 \pi(\kappa_0 + \kappa_z)}\right] e^{-2\pi(\kappa_0 - \kappa_z)}$	$2\dfrac{\sinh 2\pi\kappa_z \sinh \pi(\kappa_0 - \kappa_z)}{\sinh \pi(\kappa_0 + \kappa_z) \exp 2\pi(\kappa_0 - \kappa_z)}$
II………	$e^{-4\pi\kappa_z}$	0	$1 - e^{-4\pi\kappa_z}$
III[a]……	$\mathscr{R}_{\rm III}$	$1 - \mathscr{R}_{\rm III} - \mathscr{C}_{\rm III}$	$\mathscr{C}_{\rm III}$
IV[b]……	$1 - \mathscr{C}_{\rm IV}$	0	$\mathscr{C}_{\rm IV}$

[a] See eq. (22).
[b] See eq. (24).

4.1.2. *Incident Fast Mode*

Similarly for the incident fast wave, given by

$$u_f = a_{2\ 3} u_2 - a_{2\ 2} u_3 \tag{21}$$

in each Region, the various energy fluxes are also set out in Table 1. The associated reflection, transmission, and conversion (fast to slow) coefficients are calculated as above, tabulated in Table 3, and plotted in Figure 3. Once again, transmission cannot occur below the acoustic cutoff frequency because of the unavailability of a traveling wave at low β in this regime. In Region I though, $\mathscr{T}$ *decreases* monotonically with increasing κ to reach zero at the interface between Regions I and III. However, we also see significant transmission in the low-frequency part of Region III, due to fast mode tunnelling. The reflection, conversion, and transmission coefficients here are

$$\mathscr{R}_{\rm III} = \frac{|A\tau_- - B\tau_+|^2}{|A\tau_- + B\tau_+|^2}, \qquad \mathscr{C}_{\rm III} = \frac{D}{|A\tau_- + B\tau_+|^2},$$
$$\mathscr{T}_{\rm III} = 1 - \mathscr{R}_{\rm III} - \mathscr{C}_{\rm III}, \tag{22}$$

where

$$\tau_\pm = e^{i\pi\kappa}\text{csch}\pi(\kappa_0 \pm i|\kappa_z|) + e^{\pi\kappa_0} \sec \pi(\kappa \pm |\kappa_z|)$$

and

$$A = 2|\kappa_z||\Gamma(-|\kappa_z| - i\kappa_0)|^2\Gamma\left(\frac{1}{2} - \kappa - |\kappa_z|\right)\Gamma\left(\frac{1}{2} + \kappa - |\kappa_z|\right)\Gamma(2|\kappa_z|)^2,$$
$$B = i\pi|\Gamma(|\kappa_z| - i\kappa_0)|^2\csc(2\pi|\kappa_z|)\Gamma\left(\frac{1}{2} - \kappa + |\kappa_z|\right)\Gamma\left(\frac{1}{2} + \kappa + |\kappa_z|\right),$$
$$D = \frac{16\pi^5(1 + 2e^{2\pi\kappa_0} \cos 2\pi\kappa + e^{4\pi\kappa_0})\Gamma(2|\kappa_z|)^2}{(\kappa_0^2 + |\kappa_z|^2)(\cos 2\pi\kappa + \cos 2\pi|\kappa_z|)^2(\cos 2\pi|\kappa_z| - \cosh 2\pi\kappa_0)^2}. \tag{23}$$

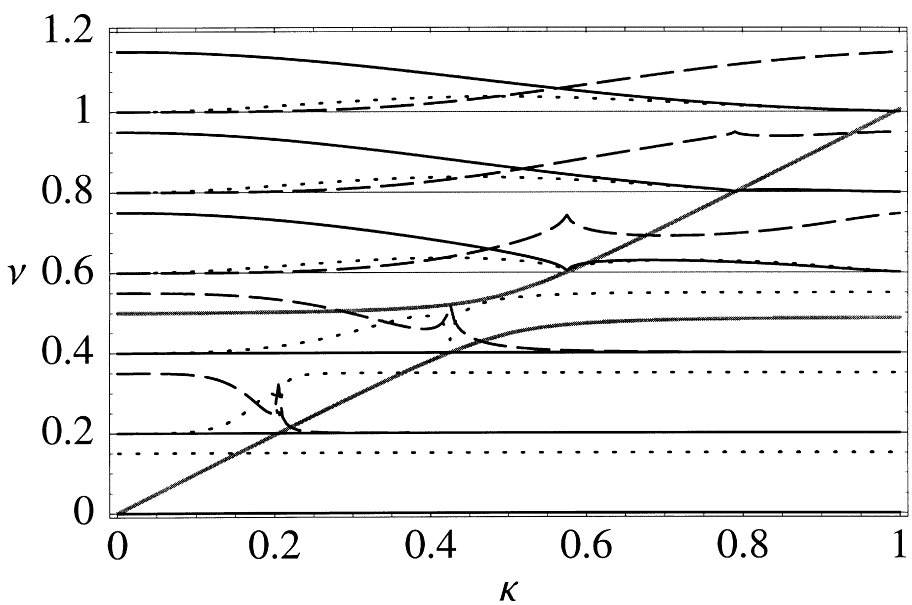

Fig. 3.—Same as Fig. 2, but for a fast wave incident from below

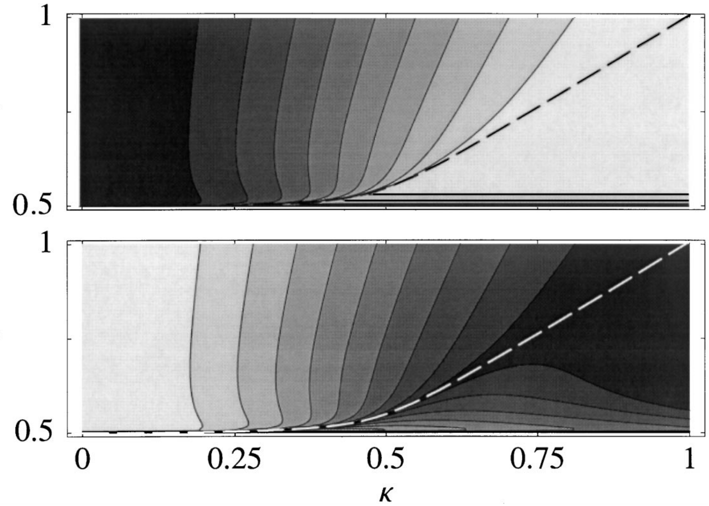

FIG. 4.—Transmission coefficients for slow (*upper panel*) and fast (*lower panel*) waves incident from below, for frequencies above the acoustic cutoff $\nu = \frac{1}{2}$ (below this, $\mathscr{T} = 0$). The contours are of $\mathscr{T} = 0.1, 0.2, \ldots, 0.9$, with the darkest shading indicating $0 < \mathscr{T} < 0.1$ and the lightest $0.9 < \mathscr{T} < 1$. The boundary curve between Regions I and III is superimposed (*dashed line*).

Finally, fast mode tunnelling in Region IV allows energy to reach up to the $\beta \approx 1$ layer, where it is converted into a downgoing slow wave (as in Region II, no transmission into the asymptotic low β region can occur). The fast-to-slow conversion coefficient may again be given exactly. Unfortunately, in this region where both κ_0 and κ_z are imaginary, the combination of gamma functions in the coefficients cannot be reduced as fully as they have been elsewhere, and rather complicated expressions result. Nevertheless, we find

$$\mathscr{C}_{\mathrm{IV}} = \frac{2\pi^5 \csc^2\pi(|\kappa_0| - |\kappa_z|)\csc^2\pi(|\kappa_0| + |\kappa_z|)\sec^2\pi(\kappa - |\kappa_z|)\sec^2\pi(\kappa + |\kappa_z|)}{|\kappa_z|(|\kappa_0|^2 - |\kappa_z|^2)\sec^2\pi(\kappa - |\kappa_0|)|E|^2}, \tag{24}$$

where

$$E = \sum_{\pm} \sqrt{\mp}\,\Gamma(\mp 2|\kappa_z|)\Gamma\left(\frac{1}{2} - \kappa \pm |\kappa_z|\right)\Gamma\left(\frac{1}{2} + \kappa \pm |\kappa_z|\right) \times \Gamma(\pm|\kappa_z| - |\kappa_0|)\Gamma(\pm|\kappa_z| + |\kappa_0|)(e^{i\pi\kappa}\csc\pi(|\kappa_0| \pm |\kappa_z|) + ie^{i\pi|\kappa_0|}\sec\pi(\kappa \pm |\kappa_z|)).$$

Then $\mathscr{T}_{\mathrm{IV}} = 0$ and $\mathscr{R}_{\mathrm{IV}} = 1 - \mathscr{C}_{\mathrm{IV}}$.

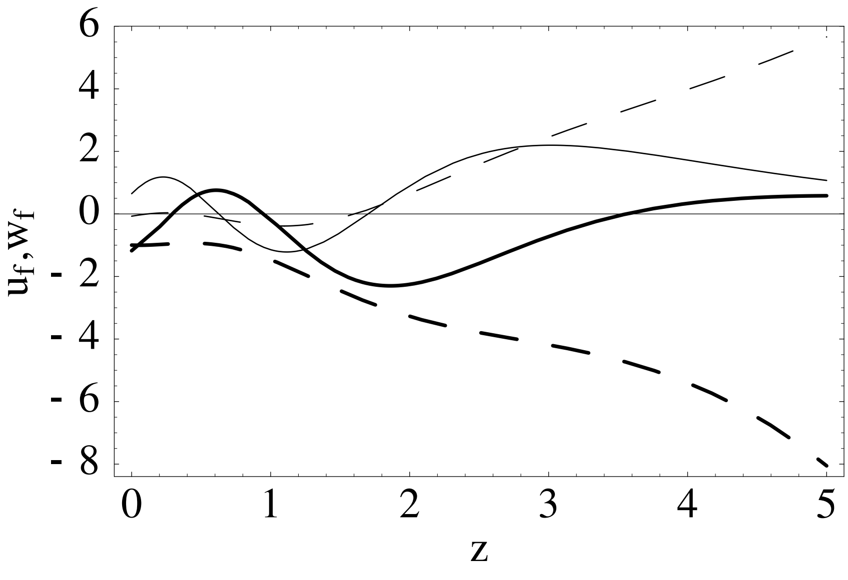

FIG. 5.—Horizontal velocity u (*solid curves*) and vertical velocity w (*dashed curves*) corresponding to an incident tunnelling fast mode with $\kappa = 0.75$, $\nu = 0.505$, i.e., near the bottom of Region III (real parts are indicated by thick lines, and the imaginary parts by thin lines). The reflection, transmission, and conversion coefficients are $\mathscr{R} = 0.014$, $\mathscr{T} = 0.425$, and $\mathscr{C} = 0.560$. The atmosphere is defined by $H = 1$ and $a(0)/c = 0.1$, so that $a = c$ at $z = 4.6$ and $\beta = 120$ at $z = 0$. Velocities are normalized so that $|w| = 1$ at $z = 0$.

Figure 4 depicts the transmission coefficients for both the incident slow mode and the incident fast mode. The effects of fast mode tunnelling in Region III are clear. Figure 5 shows the velocities for an incident tunnelling fast mode, with the downward propagating slow wave (seen most clearly in horizontal velocity) very apparent.

5. MORE COMPLEX MODELS

Solar atmospheric models consisting of two stacked isothermal layers, a "chromosphere" and a "corona," have often been adopted in wave studies (e.g., Cally 1983; Cally, Bogdan, & Zweibel 1994, which addresses the coupling of chromospheric and coronal oscillations to solar interior magnetically modified p-modes). In the top layer one would select the two physical solutions as above. The matching condition across the interface ("transition region") is that both u and w as well as their z-derivatives are continuous there (Leroy & Schwartz 1982). This allows the calculation of the C coefficients in the lower layer. All four solutions would in general be present, indicating partial reflection off the transition region. Calculation of the various reflection and transmission coefficients (which has been carried out numerically in the past using shooting methods) is trivial using the exact solutions presented in this note. We shall not pursue this further here.

6. CONCLUSION

Nontrivial exact solutions in complex magnetohydrodynamic systems are a rarity. Their value exceeds that of direct application to modeling physical systems, since they both aid in conceptual development, and provide valuable test cases for numerical simulations.

Magneto-atmospheric waves are a case in point. There is currently much interest in modeling oscillations in the solar atmosphere in response to detailed simultaneous *SOHO* observations at a range of heights (Judge, Tarbell, & Wilhelm 2000; McIntosh et al. 2000). On the real Sun, waves must contend with a variety of complex magnetic structures, such as canopy and dipole elements, but nevertheless a good understanding of the behavior of waves in a uniform vertical magnetic field and isothermal atmosphere is a crucial step toward developing a conceptual framework in which we may interpret what we see.

In this note, the simplest magneto-atmospheric wave model which includes all three restoring forces—compressibility, buoyancy, and magnetic—is revisited. Although the pioneering paper of Zhugzhda & Dzhalilov (1982) is well known, its representation of the solutions in terms of Meijer G-functions (which are defined in general by a complicated contour integral) has deterred many from using them. The fact that the particular Meijer functions used by Zhugzhda & Dzhalilov could be expressed as generalized hypergeometric functions did not seem to be appreciated. The solutions in terms of hypergeometric ${}_2F_3$ functions are less daunting, and it is hoped will find ready applicability in modeling and code testing.

As well as presenting the hypergeometric form of the solutions, we have taken the opportunity to complete the discussion of wave energy transport in a single layer isothermal magneto-atmosphere given by Zhugzhda & Dzhalilov. In particular, the new results are as follows:

1. The wave energy flux can be represented very concisely as Hermitian forms $C^H \Phi C$ or $c^H \Psi c$, where Φ and Ψ are extremely simple sparse 4×4 Hermitian matrices. Their off-diagonal terms, where present, directly represent energy transport via tunnelling.
2. In Regions III and IV of the acoustic-gravity propagation diagram, where the fast wave is evanescent at high β, tunnelling nevertheless allows energy to reach up to the $\beta \approx 1$ layer where it may be converted into a low-β fast mode and propagated upward (Region III only), or converted into a slow wave and sent back downward (both Regions). Analytic reflection, transmission, and fast-to-slow conversion coefficients are presented.

In the interests of conciseness, and in accordance with the limited intent in this note to simply present the exact solutions for use by the solar community, no detailed applications have been examined here.

REFERENCES

Bray, R. J., & Loughhead, R. E. 1974, The Solar Chromosphere (London: Chapman and Hall)
Cally, P. S. 1983, Sol. Phys., 88, 77
Cally, P. S., Bogdan, T. J., & Zweibel, E. G. 1994, ApJ, 437, 505
Ferraro, V. C. A., & Plumpton, C. 1958, ApJ, 127, 459
———. 1966, An Introduction to Magneto-fluid Mechanics (Oxford: Oxford Univ. Press)
Judge, P. G., Tarbell, T. D., & Wilhelm, K. 2000, ApJ, submitted
Lamb, H. C. 1945, Hydrodynamics (New York: Dover)
Leroy, B., & Schwartz, S. J. 1982, A&A, 112, 84
Luke, Y. L. 1974, Mathematical Functions and Their Approximations (New York: Academic Press)
McIntosh, S. W., et al. 2000, ApJL, submitted
Thomas, J. H. 1983, Ann. Rev. Fluid Mech., 15, 321
Wolfram, S. 1999, The Mathematica Book (4th ed.; New York: Cambridge Univ. Press)
Zhugzhda, Y. D. 1979, AZh, 56, 74
Zhugzhda, Y. D., & Dzhalilov, N. S. 1982, A&A, 112, 16